

# Parametric instabilities in the LCGT arm cavity

K Yamamoto<sup>1</sup>, T Uchiyama<sup>1</sup>, S Miyoki<sup>1</sup>, M Ohashi<sup>1</sup>, K Kuroda<sup>1</sup>,  
K Numata<sup>2</sup>

<sup>1</sup> Institute for Cosmic Ray Research, The University of Tokyo, Kashiwa, Chiba 277-8582, Japan

<sup>2</sup> NASA Goddard Space Flight Center, CRESST, Code663, Greenbelt, MD 20771, U.S.A.

E-mail: yamak@icrr.u-tokyo.ac.jp

**Abstract.** We evaluated the parametric instabilities of LCGT (Japanese interferometric gravitational wave detector project) arm cavity. The number of unstable modes of LCGT is 10-times smaller than that of Advanced LIGO (U.S.A.). Since the strength of the instabilities of LCGT depends on the mirror curvature more weakly than that of Advanced LIGO, the requirement of the mirror curvature accuracy is easier to be achieved. The difference in the parametric instabilities between LCGT and Advanced LIGO is because of the thermal noise reduction methods (LCGT, cooling sapphire mirrors; Advanced LIGO, fused silica mirrors with larger laser beams), which are the main strategies of the projects. Elastic Q reduction by the barrel surface (0.2 mm thickness Ta<sub>2</sub>O<sub>5</sub>) coating is effective to suppress instabilities in the LCGT arm cavity. Therefore, the cryogenic interferometer is a smart solution for the parametric instabilities in addition to thermal noise and thermal lensing.

## 1. Introduction

Observations using several interferometric gravitational wave detectors (LIGO [1], Virgo [2], GEO [3], TAMA [4]) on the ground are presently in progress. In order to construct detectors with better sensitivity, future (second generation) projects have been proposed: Advanced LIGO (U.S.A.) [5] and LCGT (Japan) [6]. These projects have km-scale Fabry-Perot cavities. The optical transversal mode spacing in these long cavities and the intervals of the elastic modes of the mirrors are on the order of 10 kHz. When the optical transversal mode spacing are comparable with the intervals of the elastic modes, parametric instabilities become a problem in the stable operation of the interferometer [7]. Small thermally driven elastic vibration modulates the light and excites the transverse modes of the cavity. These excited optical modes apply modulated radiation pressure on the mirrors. This makes the amplitude of the elastic modes larger. At last, the elastic modes and optical modes, except for TEM00, oscillate largely.

The formula of the parametric instability (without power recycling, resonant sideband extraction, and anti-Stokes modes) is derived in Ref. [7]. If a parameter,  $R$ , of an elastic mode is larger than unity, that mode is unstable. The formula of  $R$  is

$$R = \sum_{\text{optical mode}} \frac{4PQ_m Q_o}{McL\omega_m^2} \frac{\Lambda_o}{1 + \Delta\omega^2/\delta_o^2}, \quad (1)$$

where  $P, Q_m, Q_o, M, c, L, \omega_m, \Delta\omega$ , and  $\delta_o$  are the optical power in the cavity, the Q-values of the elastic and optical modes, the mass of the mirror, the speed of light, the cavity length,

the angular frequency of the elastic mode, the angular frequency differences between the elastic and optical modes, and the half-width angular frequency of the optical mode, respectively. The value  $\Lambda_o$  represents the spatial overlap between the optical and elastic modes. If the shapes of the optical and elastic modes are similar,  $\Lambda_o$  is on the order of unity. If the shapes are not similar,  $\Lambda_o$  is almost zero. When the shapes and frequencies of the optical and elastic modes are similar ( $\Lambda_o \sim 1, \Delta\omega \sim 0$ ),  $R$  will become several thousand in future projects [8]. These parametric instabilities are a serious problem in Advanced LIGO [9, 10]. The instabilities of the LCGT interferometer have never been considered. We evaluated the instabilities of the LCGT arm cavity. In Sec. 2, we introduce the calculation results for the parametric instabilities in LCGT and compare them with those in Advanced LIGO. In order to calculate  $\omega_m$  and  $\Lambda_o$  for the instability evaluation, we used ANSYS, which is a software application for a finite-element method [11]. In Sec. 3, the difference in the parametric instabilities between Advanced LIGO and LCGT is discussed. In Sec. 4, how to suppress the instabilities of the LCGT arm cavity is considered. Sec. 5 and Sec. 6 are devoted to future work and a summary, respectively.

## 2. Results of calculation

### 2.1. Specification

Table 1 gives the specifications of Advanced LIGO in Refs. [9, 10, 12] (after these references, the specifications of Advanced LIGO were changed slightly) and LCGT [13] (the exact values of the LCGT mirror curvature are not fixed. The curvature given in Table 1 is only a candidate). The important differences between Advanced LIGO and LCGT are in the mirror curvature radius, beam radius, mirror material and temperature.

**Table 1.** Specification of Advanced LIGO [9, 10, 12] and LCGT [13].

	Advanced LIGO	LCGT
Laser beam profile	Gaussian	Gaussian
Wavelength	1064 nm	1064 nm
Cavity length	4000 m	3000 m
Front mirror curvature radius	2076 m	7114 m
End mirror curvature radius	2076 m	7114 m
Beam radius at the mirrors	60 mm	35 mm
Power in a cavity	0.83 MW	0.41 MW
Mirror material	Fused silica	Sapphire
Mirror mass	40 kg	30 kg
Mirror temperature	300 K	20 K

### 2.2. Advanced LIGO

We briefly overview an estimation of the instabilities in Advanced LIGO by a group at the University of Western Australia [9, 10] for an easier comparison. They investigated what happens when the curvature of a mirror is changed. The curvature of the other mirror is the default value given in Table 1. Figure 1(c) of Ref. [10] shows the curvature dependence of the unstable mode number. The crosses in this figure represent the cavities, which consist of the fused-silica mirrors. The number of unstable modes is between 20 and 60. Figure 5 of Ref. [9] shows that the maximum of  $R$  in the various elastic modes strongly depends on the mirror curvature. Even a shift of only a few meters in the mirror curvature causes a drastic change of the maximum  $R$ .

The requirement of the accuracy in the mirror curvature in Advanced LIGO is difficult to be achieved.

### 2.3. LCGT

We investigated the parametric instabilities of the LCGT arm cavity in the same manner as that of the University of Western Australia. Figure 1 shows the mirror curvature dependence of the unstable mode number in the LCGT arm cavity. The number is only 2 ~ 4, which is 10-times smaller than that of Advanced LIGO. Figure 2 shows that the mirror curvature dependence of the maximum  $R$  is weaker than that of Advanced LIGO. The maximum  $R$  is not changed drastically by a shift of a few meters in the mirror curvature. It is easier to satisfy the requirement of the mirror curvature in LCGT. It must be noticed that the power recycling was not taken into account in our calculation. The evaluation of Advanced LIGO included the power recycling effect. The difference between the maximums of  $R$  with and without the power recycling is shown in fig. 2 of Ref. [10]. Although the peaks of the maximum  $R$  become higher owing to the power recycling, this is not a serious effect on the discussion about the difference between Advanced LIGO and LCGT in the next section.

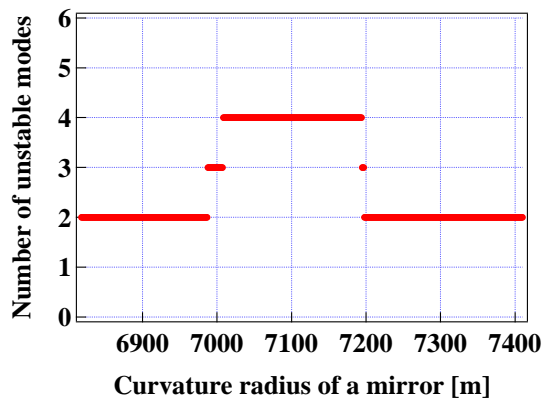


**Figure 1.** Number of unstable modes in the LCGT arm cavity. The horizontal axis is the curvature radius of a mirror. The curvature of the other mirror is the default value given in Table 1. This graph corresponds to fig. 1(c) of Ref. [10] for Advanced LIGO.

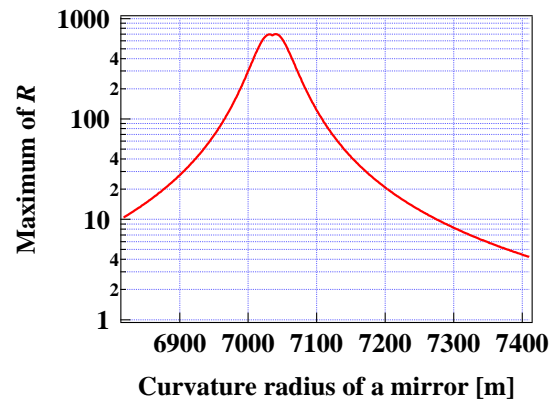


**Figure 2.** Maximum of  $R$  in the various elastic modes in the LCGT arm cavity. The horizontal axis is the curvature radius of a mirror. The curvature of the other mirror is the default value given in Table 1. This graph corresponds to fig. 5 of Ref. [9] for Advanced LIGO.

## 3. Discussion

Our investigation revealed that there is the large difference in the parametric instabilities between Advanced LIGO and LCGT. We discuss the reasons in this section.

### 3.1. Number of unstable modes

The difference in the unstable mode numbers originates from the mode frequency density difference. If both of the optical and elastic mode densities are large, the optical mode frequencies often coincide with the elastic mode frequencies. The elastic mode density is inversely proportional to the cube of the sound velocity in the material. The sound velocities of the fused silica (Advanced LIGO) and sapphire (LCGT) are about 6 km/sec and 10 km/sec, respectively. The elastic mode density of LCGT is 5-times smaller. In Advanced LIGO, there are 7 optical

transverse modes in a free spectrum range [9]. On the contrary, there are only 3 modes in the LCGT arm cavity. The optical mode density of LCGT is 2-times smaller. The larger optical mode density of Advanced LIGO stems from a larger beam radius adapted for suppressing the mirror thermal noise [5]. In LCGT, since the mirrors are cooled in order to reduce the thermal noise [6], larger beams are not necessary. As a result, the product of the elastic and optical mode densities of LCGT becomes 10-times smaller. In fact, the unstable mode number calculated by us for LCGT ( $2 \sim 4$  in fig. 1) is 10-times less than that calculated at the University of Western Australia for Advanced LIGO ( $20 \sim 60$  in fig. 1(c) of Ref. [10]).

### *3.2. Mirror curvature dependence*

In LCGT, the maximum value of  $R$  depends on the mirror curvature more weakly. This implies that the curvature dependence of the optical mode frequencies is weaker, because  $R$  is a function of the optical mode frequencies. We calculated how the curvature variation affects the  $n$ -th optical transverse mode. The results were  $15n$  Hz/m in Advanced LIGO and  $0.58n$  Hz/m in LCGT. LCGT shows a 30-times weaker dependence due to the larger optical transversal mode spacing, which stems from the smaller beam radius.

### *3.3. Summary of discussion*

The difference in the parametric instabilities between Advanced LIGO and LCGT is caused by those of the beam radii (Advanced LIGO, 60 mm; LCGT, 35 mm) and the mirror materials (Advanced LIGO, fused silica; LCGT, sapphire). These differences mostly originate from that of the thermal noise-reduction methods (Advanced LIGO, fused silica mirrors with larger laser beams; LCGT, cooling sapphire mirrors), which are the main strategies of the projects [5, 6]. The cryogenic interferometer has an advantage in the parametric instabilities (less unstable mode number and weaker dependence on the mirror curvature) in addition to the small thermal noise [14, 15, 16] and negligible thermal lensing [17].

## **4. Instability suppression for LCGT arm cavity**

We showed that the unstable modes of LCGT are less than those of Advanced LIGO. Still, the LCGT arm cavity is unstable because there always exist unstable modes, as shown in fig. 1. We must consider how to suppress the instabilities. The three methods for instability suppression in Advanced LIGO are being studied at the University of Western Australia [10, 18]. We checked whether these three methods (thermal tuning method, feedback control, Q reduction of elastic modes) are appropriate for LCGT (the tranquilizer cavity [19] is one of the other methods). However, this is difficult).

### *4.1. Thermal tuning method*

In the thermal tuning method [10], a part of the mirror is heated for curvature control. Since  $R$  depends on the curvature, the suppression of  $R$  should be possible by this manner. However, this method is not useful in LCGT. First of all,  $R$  weakly depends on the mirror curvature, as shown in fig. 2 in the case of LCGT. Second, owing to the small thermal expansion and high thermal conductivity [17] of cold sapphire, the mirror curvature would not change effectively, even if we apply heat to the mirror.

### *4.2. Feedback control*

It is possible to control the light or the mirror so that the parametric instabilities would be actively suppressed [10]. If the number of unstable modes is smaller, feedback control is easier. However, these are more difficult (active) methods than Q reduction (passive method) of the elastic modes.

### 4.3. $Q$ reduction of elastic modes

This is a useful method [18] for LCGT. The value of  $R$  is proportional to the  $Q$ -value of the elastic mode,  $Q_m$ , as shown in Eq. (1). The  $Q$ -values of sapphire are about  $10^8$  [14]. The maximum  $R$  of LCGT is several hundreds at most, as shown in fig. 2. If the  $Q$ -values of the LCGT mirrors become  $10^6$ , almost all modes become stable. Since the mechanical loss concentrated far from the beam spot has a small contribution to the thermal noise [20, 21], we should be able to apply additional loss on a barrel surface, as in fig. 3, without sacrificing the thermal noise [18, 22]. Moreover, it is possible to introduce a 15-times larger loss in the LCGT mirror than that in Advanced LIGO mirror, because the LCGT mirrors are cooled (20 K) [6]. We concluded that the thermal noise of the barrel surface loss is comparable with that of the reflective-coating loss [16, 21], when the LCGT mirror  $Q$ -values become  $10^6$  owing to the additional loss. Since the reflective-coating thermal noise is smaller than the goal sensitivity of LCGT [16], this barrel surface loss is not a serious problem.

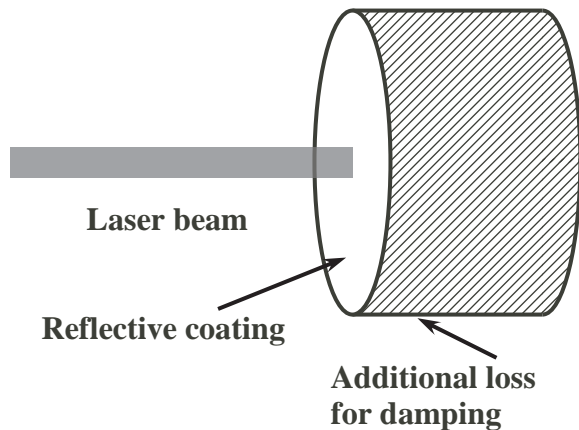


**Figure 3.** Loss on the barrel surface. Although this loss decreases the elastic  $Q$ -values of the mirror,  $Q_m$ , it has only a small contribution to the thermal noise [20, 21]. Thus, this loss suppresses the parametric instabilities without an increase of the thermal noise [18, 22].

We are able to introduce loss on the barrel surface by coating  $\text{Ta}_2\text{O}_5$ , which is a popular material for the reflective coating of the mirror. Our recent measurement [16] proved that the loss angle of the  $\text{SiO}_2/\text{Ta}_2\text{O}_5$  coating is  $(4 \sim 6) \times 10^{-4}$  between 4 K and 300 K. Since the loss of this coating is dominated by that of  $\text{Ta}_2\text{O}_5$  [23], the loss angle of  $\text{Ta}_2\text{O}_5$  is  $(8 \sim 12) \times 10^{-4}$ . If the barrel loss dominates the mirror  $Q$ , it would be expressed as [21]

$$\frac{1}{Q_m} \sim \frac{E_{\text{Ta}_2\text{O}_5}}{E_{\text{sapphire}}} \frac{2d}{R} \phi, \quad (2)$$

where  $E_{\text{Ta}_2\text{O}_5}$ ,  $E_{\text{sapphire}}$ ,  $d$ ,  $R$ ,  $\phi$  are the Young's moduli of  $\text{Ta}_2\text{O}_5$  and the sapphire, the thickness of the  $\text{Ta}_2\text{O}_5$  layer, the mirror radius and the loss angle of  $\text{Ta}_2\text{O}_5$ , respectively. These values are summarized in Table 2 [16]. In order to make the  $Q$ -values,  $Q_m$ ,  $10^6$ , the  $\text{Ta}_2\text{O}_5$  coating thickness,  $d$ , must be 0.2 mm.

**Table 2.** Specification of the coating [16].

Young's modulus of the $\text{Ta}_2\text{O}_5$ ( $E_{\text{Ta}_2\text{O}_5}$ )	$1.4 \times 10^{11}$ Pa
Young's modulus of the sapphire ( $E_{\text{sapphire}}$ )	$4.0 \times 10^{11}$ Pa
Mirror radius ( $R$ )	12.5 cm
Loss angle of $\text{Ta}_2\text{O}_5$ ( $\phi$ )	$10^{-3}$

## 5. Future work

In our calculations for this article, we took only the elastic modes below 100 kHz and the first three transverse optical modes into account. We were calculating higher elastic and optical modes. Our preliminary result suggests that there are unstable higher modes. However, the elastic Q reduction would work more effectively because the typical  $R$  still seems to be small. We must evaluate the Q reduction technique more carefully for instability suppression. The effects of power recycling [8], resonant sideband extraction [24, 25] and the anti-Stokes modes [26] must be evaluated as well.

## 6. Summary

We evaluated the parametric instabilities of LCGT and compared them with those of Advanced LIGO [9, 10]. The number of unstable elastic modes in LCGT is 10-times smaller. Since the strength of the parametric instabilities in LCGT more weakly depends on the mirror curvature, the requirement of the accuracy in the mirror curvature of LCGT is easier to satisfy. These differences in the parametric instabilities between LCGT and Advanced LIGO are made by those of the laser beam sizes and mirror materials, which mostly stem from the thermal-noise suppression strategies in both projects (LCGT, cooling sapphire mirrors; Advanced LIGO, fused silica mirrors with larger laser beams) [5, 6]. The elastic Q reduction [18] by the barrel surface (0.2 mm thickness  $\text{Ta}_2\text{O}_5$ ) coating is effective for instability suppression in the LCGT arm cavity. Thus, the cryogenic interferometer is a smart solution for the parametric instabilities in addition to the thermal noise [14, 15, 16] and thermal lensing [17].

## Acknowledgments

We are grateful to M Ando for information about candidates of the LCGT mirror curvature radius.

## References

- [1] Abramovici A *et al* 1992 *Science* **256** 325
- [2] Bradaschia C *et al* 1990 *Nucl. Instrum. Methods Phys. Res. Sect. A* **289** 518
- [3] Willke B *et al* 2002 *Class. Quantum Grav.* **19** 1377
- [4] Ando M *et al* 2001 *Phys. Rev. Lett.* **86** 3950
- [5] Wilkinson C A 2008 *Proc. the 7th Edoardo Amaldi Conference* (Bristol: Institute of Physics Publishing)
- [6] Kuroda K 2008 *Proc. of the 7th Edoardo Amaldi Conference* (Bristol: Institute of Physics Publishing)
- [7] Braginsky V B, Strigin S E and Vyatchanin S P 2001 *Phys. Lett. A* **287** 331
- [8] Braginsky V B, Strigin S E and Vyatchanin S P 2002 *Phys. Lett. A* **305** 111
- [9] Ju L, Gras S, Zhao C, Degallaix J and Blair D G 2006 *Phys. Lett. A* **354** 360
- [10] Ju L, Zhao C, Gras S, Degallaix J, Blair D G, Munch J and Reitze D H 2006 *Phys. Lett. A* **355** 419
- [11] ANSYS, Inc. Southpointe 275 Technology Drive Canonsburg, PA 15317, U.S.A. (<http://www.ansys.com/>)
- [12] Zhao C, Ju L, Degallaix J, Gras S and Blair D G 2005 *Phys. Rev. Lett.* **94** 121102
- [13] Kuroda K *et al* 2006 *Prog. Theor. Phys. Suppl.* **163** 54
- [14] Uchiyama T *et al* 1999 *Phys. Lett. A* **261** 5
- [15] Uchiyama T *et al* 2000 *Phys. Lett. A* **273** 310
- [16] Yamamoto K *et al* 2006 *Phys. Rev. D* **74** 022002
- [17] Tomaru T *et al* 2002 *Class. Quantum Grav.* **19** 2045
- [18] Gras S, Zhao C, Ju L and Blair D G 2006 *J. Phys.: Conf. Ser.* **32** 251
- [19] Braginsky V B and Vyatchanin S P 2002 *Phys. Lett. A* **293** 228
- [20] Levin Yu 1998 *Phys. Rev. D* **57** 659
- [21] Yamamoto K, Ando M, Kawabe K and Tsubono K 2002 *Phys. Lett. A* **305** 18
- [22] Gras S, Blair D G and Ju L 2004 *Phys. Lett. A* **333** 1
- [23] Penn S D *et al* 2003 *Class. Quantum Grav.* **20** 2917
- [24] Gurkovsky A G, Strigin S E and Vyatchanin S P 2007 *Phys. Lett. A* **362** 91
- [25] Strigin S E and Vyatchanin S P 2007 *Phys. Lett. A* **365** 10
- [26] Kells W and D'Ambrosio E 2002 *Phys. Lett. A* **299** 326